

Catalytic Activity of $\text{La}_{1-x}\text{Ca}_x\text{CoO}_{3-\delta}$ Perovskites ($x = 0-1$) Prepared by the Pechini Method in the Reaction of Deep Methane Oxidation

L. A. Isupova^{a, *}, N. A. Kulikovskaya^a, N. F. Saputina^a, and E. Yu. Gerasimov^a

^a*Boreshkov Institute of Catalysis, Siberian Branch, Russian Academy of Sciences, Novosibirsk, 630090 Russia*

**e-mail: isupova@catalysis.ru*

Received October 2, 2017

Abstract—The catalytic activity of a series of the perovskite-like oxides $\text{La}_{1-x}\text{Ca}_x\text{CoO}_{3-\delta}$ ($x = 0-1$) prepared by the Pechini method (from polymer–salt compositions) in the reaction of methane oxidation was studied. The dependence of the activity and stability of samples on their composition and reaction temperature was revealed. It was found that an increase in the calcium content of the oxides initially led to an increase in the activity (to the values of $x = 0.3$) and then to a nonmonotonic decrease with an intermediate maximum at $x = 0.6$. A decrease in the activity of oxides in the course of testing, which was most pronounced in the samples with $x = 0.3, 0.6$, and 1, was found. The phase compositions, specific surface areas, and microstructures of the oxides were determined before and after tests. According to X-ray diffraction analysis data, only the samples with $x = 0-0.4$ were single-phase ones; the samples with $x > 0.4$ were two-phase samples containing the phases of perovskite and brownmillerite. With the use of high-resolution transmission electron microscopy, it was found that the surface of particles was covered with the nanosized particles of simple calcium and cobalt oxides, and the particles of brownmillerite were present in the samples with $x \geq 0.4$. The observed increase in the catalytic activity of the samples in a region to $x = 0.3$ correlated with an increase in the concentration of weakly bound oxygen in the perovskites, and a decrease at $x > 0.3$, with the appearance of the less active phase of brownmillerite in the samples and an increase in its concentration. The phase composition and the specific surface area of the samples remained unchanged after tests; however, planar defects were detected in the particles of perovskite and the calcium content on the surface increased. This was caused by the appearance and ordering of cationic and anionic vacancies under the action of a reaction medium, which can explain the observed changes in the activity of the samples.

Keywords: $\text{La}_{1-x}\text{Ca}_x\text{CoO}_{3-\delta}$, perovskites, methane oxidation, stability

DOI: 10.1134/S0023158418040031

INTRODUCTION

The $\text{La}_{1-x}\text{M}_x\text{CoO}_{3-\delta}$ oxides ($M = \text{Ca}, \text{Sr}, \text{and Ba}$) with the structure of perovskite are promising materials to be used in a number of high-temperature processes. For example, they can be used in high-temperature electrochemical devices, gas sensors, oxygen-permeable membranes, etc. [1–3]. The $\text{La}_{1-x}\text{M}_x\text{CoO}_{3-\delta}$ solid solutions also acquired a good reputation as catalysts for the deep oxidation of hydrocarbons, ammonia, and CO and other processes [4–7].

It is well known that the physicochemical properties of substituted perovskites considerably depend on both the degree of substitution and the preparation conditions, which are responsible for the phase composition, microstructure, and structure imperfection of oxides. This can be a reason for differences in published data on not only the properties but also the phase composition of the oxides [8–18].

Thus, it was found that the region of formation of homogeneous solid solutions upon substitution in the $\text{La}_{1-x}\text{Ca}_x\text{CoO}_{3-\delta}$ system on ceramic synthesis was extended as the heat treatment temperature was increased. The heat treatment of initial reagents at a temperature of 885°C made it possible to obtain single-phase samples only in a range of $x = 0-0.25$ [8] or to the values of $x < 0.4$ at 1100°C [9, 10]; this is consistent with the statement of Mastin et al. [11] on the impossibility of preparing solutions with $x > 0.3$ by a ceramic method (1100°C). According to Kononyuk et al. [12], an increase in the temperature of annealing to 1200°C increased the boundary of solubility to $x = 0.5$.

The synthesis of samples from solutions makes it possible to obtain homogeneous solid solutions with a higher degree of substitution at lower calcination temperatures [11]. The following single-phase samples were studied: compositions with $x = 0-0.3$ prepared by a ceramic method ($T_{\text{calc}} = 1100^\circ\text{C}$) and composi-

tions with $x = 0.4$ and 0.5 prepared by a polymer–salt precursor method ($T_{\text{calc}} = 900^\circ\text{C}$). All of the substituted samples contained an impurity of CaO. The samples with $x = 0$ and 0.5 at room temperature were identified as a rhombohedral modification, whereas the samples with $x = 0.2$ – 0.4 , as an orthorhombic modification. At a temperature higher than 200°C , the samples with $x = 0.2$ – 0.4 became rhombohedral and the sample with $x = 0.5$ became cubic. It was shown that the temperature of a polymorphic transition to the cubic modification decreased with the calcium content of oxides from 1600°C for the sample with $x = 0$ to 20°C for the sample with $x = 0.5$. Mastin et al. [11] also established that the concentration of oxygen vacancies in the oxides increased with the quantity of calcium, and the stability on heating in nitrogen decreased. The latter led to a decrease in the calcium content of the perovskite phase and the appearance of layered perovskite phases of $(\text{La,Ca})_2\text{CoO}_4$ and CoO .

Melo et al. [13] used a polymer–salt precursor method to synthesize the $\text{La}_{1-x}\text{Ca}_x\text{CoO}_{3-\delta}$ perovskites with $x = 0$ – 0.4 . They found that the heat treatment of the samples at 700°C in air for 4 h facilitated the formation of almost single-phase perovskites with a rhombohedral structure. They demonstrated that, in contrast to the data reported by Mastin et al. [11], an increase in the calcination temperature to 800 and 900°C led to the formation of cubic perovskite in the sample with $x = 0.4$.

Pathak et al. [14] established that the samples with $x = 0.4$ and 0.55 contained the impurities of calcium and cobalt oxides in addition to the rhombohedral phase of perovskite; this fact is indicative of the formation of limited solid solutions in the system to the values of $x = 0.4$.

At the same time, Kumar et al. [17] stated that single-phase samples with the values of $x = 0$ – 0.8 were obtained from the polymer–salt precursors after their heat treatment at 900°C for 12 h. The samples with $x = 0$ and 0.2 were identified as a rhombohedral modification, while the samples with $x \geq 0.4$, as a cubic modification. Kumar et al. [17] noted a decrease in particle sizes with the calcium content of the oxides and a decrease in electron density on oxygen ions. The single-phase samples with $x = 0$ – 0.8 were also synthesized by a citrate method after heat treatment at 700 – 750°C ; it was shown that cobalt in the oxides had the oxidation state close to $+3$, and vacancies were formed in the oxides upon substitution [18].

Merino with coauthors [15, 16] studied the catalytic properties of single-phase perovskites with $x = 0$ – 0.5 prepared by the citrate method (heat treatment at 700°C for 2 h). The oxides were characterized as a rhombohedral modification. The presence of a lanthanum oxide impurity, which cannot be detected by X-ray diffraction analysis, on the surfaces of all samples was found. The authors of the cited publications revealed an increase in the concentration of oxygen

vacancies upon the introduction of calcium into the perovskites and a nonmonotonic change in activity in the oxidation reaction of propane at temperatures of 140 – 420°C . At $x = 0.2$, the activity of perovskite ($\text{La}_{0.8}\text{Ca}_{0.2}\text{CoO}_3$) with respect to lanthanum cobaltite decreased or increased at a larger quantity of calcium. The found order of activity— $\text{La}_{0.6}\text{Ca}_{0.4}\text{CoO}_3 > \text{LaCoO}_3 > \text{La}_{0.8}\text{Ca}_{0.2}\text{CoO}_3$ —did not correlate with an increase in the concentration of vacancies in the oxides. The authors of the above publications reported the high stability of the samples in a reaction medium. Unfortunately, other data on the catalytic oxidation of hydrocarbons on the above oxides are absent from the literature.

Discordance between published data on the phase composition of the $\text{La}_{1-x}\text{Ca}_x\text{CoO}_{3-\delta}$ perovskites prepared by different methods can be caused by different conditions of their synthesis (the degree of homogenization of the components at the stage of mixing and the duration and atmosphere of the subsequent heat treatment) and by a possible decrease in the solubility of calcium with the temperature of heat treatment because of the ordering of oxygen vacancies by analogy with the $\text{La}_{1-x}\text{Ca}_x\text{FeO}_{3-\delta}$ system studied previously [19–21]. Furthermore, with consideration for data on the stability of the $\text{La}_{1-x}\text{Ca}_x\text{CoO}_{3-\delta}$ perovskites on heating in nitrogen [11], it is reasonable to study their stability in a reaction medium containing reducing agents at higher catalytic process temperatures than those used by Merino with coauthors [15, 16]. Thus, the degradation of perovskites with $x > 0.3$ (predominantly in the near-surface layers of oxides) under the action of a methane-containing reaction atmosphere was observed earlier even in the $\text{La}_{1-x}\text{Ca}_x\text{MnO}_3$ system [22–24].

The polymer–salt precursor method is widely used for the synthesis of multicomponent solid solutions. Because of the good homogenization of components at the stage of precursor preparation, the complete degree of interaction is reached at sufficiently low temperatures and short calcination times in comparison with those in the ceramic method. The advantages of the method over a precipitation method include the absence of wastewater to be utilized.

The aim of this work was to prepare a wide range of $\text{La}_{1-x}\text{Ca}_x\text{CoO}_{3-\delta}$ ($x = 0$ – 1) homogeneous solid solutions by the polymer–salt precursor method, to determine their physicochemical and catalytic properties in a reaction of methane oxidation, and to study their stability in the reaction medium.

EXPERIMENTAL

The samples of $\text{La}_{1-x}\text{Ca}_x\text{CoO}_{3-\delta}$ were synthesized by the polymer–salt composition method (the Pechini method). For this purpose, the aqueous solutions of lanthanum, calcium, and cobalt nitrates were mixed in a required proportion, and citric acid and

ethylene glycol were added; the contents were evaporated at 70–80°C until the formation of a resinous polymer (polymer–salt composition). After the oxidative destruction of the polymer, the resulting product was calcined at 900°C for 4 h.

The X-ray diffraction patterns of the samples were measured on an HZG 4-C diffractometer (Freiberger Präzisionsmechanik, Germany) with the use of $\text{CuK}\alpha$ radiation on scanning with a step of $2\theta = 0.05^\circ$ point by point and an accumulation time of 3 s at each point in a range of the angles $2\theta = 10^\circ\text{--}75^\circ$.

The high resolution (to 1.4 Å) electron microscopic images were obtained on a JEM-2010 instrument (JEOL, Japan). The X-ray microanalysis (EDX) of the elemental composition of the samples was carried out with the use of a Phoenix energy-dispersive spectrometer (EDAX, the United States) with a Si(Li) detector at an energy resolution of 130 eV.

The temperature-programmed reduction with hydrogen (TPR- H_2) was carried out in a flow system with a thermal conductivity detector using a sample fraction of 0.25–0.5 mm. Before the reduction, the samples were trained in O_2 for 0.5 h at 500°C and then cooled in O_2 to room temperature. The sample weight was 10 mg, and the flow rate of a reducing mixture (10% H_2 in Ar) was 40 cm^3/min . The samples were heated to 900°C at a rate of 10 K/min. The peak areas under the TPR curves of the samples, which corresponded to the consumption of hydrogen (mole per gram of the sample), was calculated using the Origin 6.0 software.

The catalytic activity of the samples in a reaction of methane oxidation was determined in a flow system at temperatures of 350–600°C. A 1-g portion of a catalyst fraction of 0.25–0.5 mm was mixed with 1 cm^3 of quartz and placed in a U-shaped quartz reactor with an inside diameter of 4.5 mm. The feed rate of a reaction mixture of 0.9% $\text{CH}_4 + 9\% \text{O}_2$ (and the balance N_2) was 2.4 L/h. Before the measurements, the sample was kept in the reaction mixture for ~30 min at a specified temperature. After testing at 600°C, the sample was cooled in the reaction mixture to 500°C and its activity was determined once again. Only carbon dioxide and water were the oxidation products of methane.

The reaction rate w was calculated under the assumption that the reaction occurred in a plug-flow regime using the formula

$$w = 2.69 \times 10^{19} k C_0, (\text{CH}_4 \text{ molecule}) \text{m}^{-2} \text{s}^{-1},$$

where C_0 is the initial concentration of methane, %; k is the reaction rate constant $k = \ln(1 - X_{\text{CH}_4}) / (\tau S_{\text{sp}} m)$, $\text{m}^{-2} \text{s}^{-1}$ (X_{CH_4} is the degree of methane conversion; τ is the contact time, s; m is the sample weight, g; and S_{sp} is the specific surface area of the sample, m^2/g).

The specific surface area was measured by the BET method based on the thermal desorption of argon.

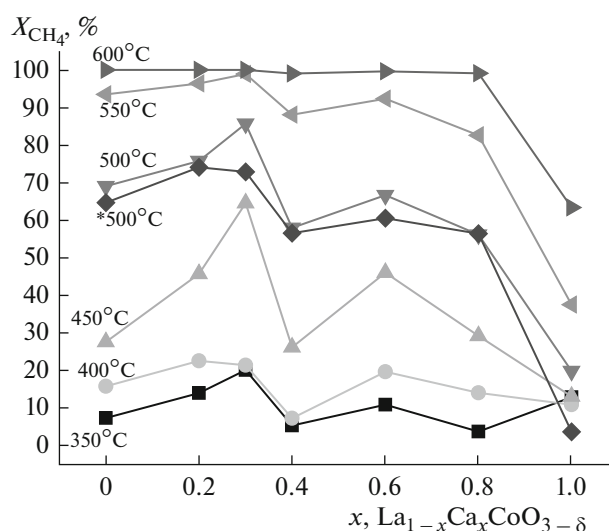


Fig. 1. Dependence of the conversion of methane on the calcium content (x) of the $\text{La}_{1-x}\text{Ca}_x\text{CoO}_{3-\delta}$ oxides at testing temperatures of 350–600°C. * The experiment was carried out after sample testing at 600°C and the subsequent decrease of temperature to 500°C.

RESULTS AND DISCUSSION

Figures 1 and 2 illustrate data on the conversion and the rate of oxidation of methane for the test samples. It is evident that the activity of all of the samples increased with the test temperature, and the conversion of methane reached 100% at 600°C for all of the oxides other than those with $x = 1$.

In a temperature range of 350–550°C, an increase in the calcium content of the samples was accompanied by a nonmonotonic change in conversion with maximums at $x = 0.3$ and 0.6 , which were most pronounced at $T = 450\text{--}500^\circ\text{C}$. The dependence of the reaction rate of methane oxidation on the composition of oxides had an analogous form (Fig. 2). The repeated determination of the activity of samples after a temperature decrease from 600 to 500°C revealed a noticeable decrease in the activity of samples with $x = 0.3$ and $x = 0.6$ (the samples with maximum initial activities) and also a sample with $x = 1$.

The determination of the specific surface areas of the samples before and after tests did not reveal changes within the limits of measurement error (Table 1). The specific surface area of all of the substituted samples before and after tests was $3 \pm 0.5 \text{ m}^2/\text{g}$. The specific surface area of unsubstituted lanthanum cobaltite ($x = 0$) was higher ($5.1\text{--}5.8 \text{ m}^2/\text{g}$).

The experimental data that are indicative of the influence of the calcium content of the samples on the activity and a decrease in the activity of some catalysts in the course of tests cannot be explained by the specific surface areas of the catalysts. The substituted samples, which were characterized by a higher degree of methane conversion than that on unsubstituted lan-

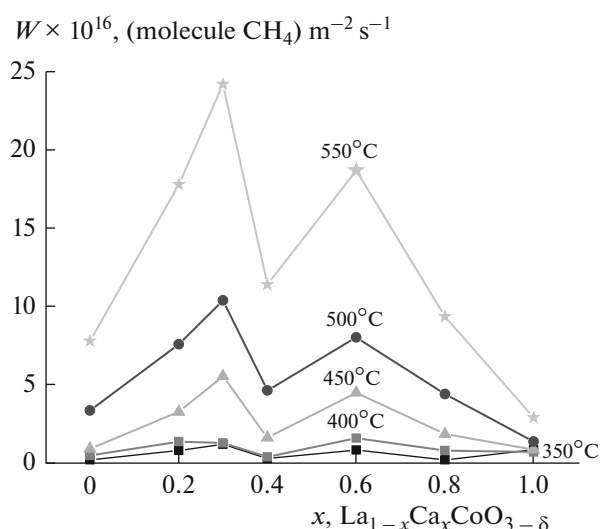


Fig. 2. Dependence of the reaction rate of methane oxidation on the calcium content (x) of the $\text{La}_{1-x}\text{Ca}_x\text{CoO}_{3-\delta}$ oxides at testing temperatures of 350–550°C.

thanum cobaltite (the samples with $x = 0.2, 0.3, 0.6$, and 0.8), possessed a smaller specific surface area, and their surface was not decreased after tests. This fact indicates that a change in the chemical composition of the surface of oxides in the course of tests can be the reason for the observed decrease in the activity of the samples.

According to the X-ray diffraction (XRD) analysis data (Fig. 3), the samples of $\text{La}_{1-x}\text{Ca}_x\text{CoO}_{3-\delta}$ to $x = 0.4$ before the catalytic tests were almost single-phase homogeneous solid solutions. The introduction of calcium leads to a decrease in unit cell parameters (Table 1), which is consistent with published data [17]. The samples with $x = 0-0.2$ belong to the rhombohedral symmetry R-3c ($x = 0$) and R-3m ($x = 0.2$) (JCPDS 48-123

and 36-1388, respectively), and the sample with $x = 0.4$, to the cubic Pm3-m symmetry (JCPDS 36-1391). The sample with $x = 0.3$ exhibited the peaks of perovskite phases with the orthorhombic (R-3m) and cubic (Pm-3m) symmetry. Starting with $x = 0.4$, a $\text{Ca}_2\text{Co}_2\text{O}_5$ phase impurity with the structure of brownmillerite appeared in the samples, and its amount increased with x ; in this case, the composition of the perovskite phase remained unchanged, and its parameter corresponded to $\text{La}_{0.6}\text{Ca}_{0.4}\text{CoO}_{3-\delta}$. The phases of $\text{Ca}_3\text{Co}_2\text{O}_6$ and CaO were also detected among the impurities. The sample of $\text{CaCoO}_{3-\delta}$ predominantly consisted of the two phases: $\text{Ca}_3\text{Co}_4\text{O}_9$ and $\text{Ca}_3\text{Co}_2\text{O}_6$; the presence of a CaO impurity phase also cannot be excluded. Figure 4 shows changes in the volume of a unit cell upon the introduction of calcium. A decrease in the unit cell volume observed in fresh samples (Fig. 4) indicates that calcium entered into the lattice of perovskite with the formation of a limited number of solid solutions in the system, in contrast to published data [17, 18].

Thus, in accordance with the XRD analysis data, almost single-phase solid solutions were formed on the introduction of calcium only to $x = 0.4$; in this case, a change in their structural modification was observed; therefore, the sample with $x = 0.3$ can be attributed to the region of a morphotropic phase transition.

The phase composition of single-phase samples with $x = 0-0.4$ remained unchanged after catalytic tests in the reaction of methane oxidation (Fig. 5), although it was possible to note an insignificant increase in the unit cell volume (Fig. 4), which was likely caused by the appearance of oxygen vacancies in the samples and, possibly, by a decrease in the calcium content.

Figure 6 shows the TPR- H_2 curves. The reduction of samples by hydrogen with an increase in the tem-

Table 1. Specific surface areas and unit cell parameters of the samples of $\text{La}_{1-x}\text{Ca}_x\text{CoO}_{3-\delta}$ before and after catalytic tests in the reactions of methane oxidation

Catalyst composition	$S_{\text{sp}}, \text{m}^2/\text{g}$		Unit cell parameters of the initial samples		Unit cell parameters of the samples after the oxidation of CH_4	
	initial	after the oxidation of CH_4	$a, \text{Å}$	$c, \text{Å}$	$a, \text{Å}$	$c, \text{Å}$
$\text{LaCoO}_{3-\delta}$	5.6	5.1	5.4402	13.0807	5.4471	13.0996
$\text{La}_{0.8}\text{Ca}_{0.2}\text{CoO}_{3-\delta}$	3.0	3.5	5.4168	13.0836	5.4336	13.1205
$\text{La}_{0.7}\text{Ca}_{0.3}\text{CoO}_{3-\delta}$	3.0	—	5.4154	13.0946	—	—
$\text{La}_{0.6}\text{Ca}_{0.4}\text{CoO}_{3-\delta}$	3.0	1.9	3.787	3.787	3.816	3.816
$\text{La}_{0.4}\text{Ca}_{0.6}\text{CoO}_{3-\delta}$	2.2	—	—	—	—	—
$\text{La}_{0.2}\text{Ca}_{0.8}\text{CoO}_{3-\delta}$	3.0	—	—	—	—	—
$\text{CaCoO}_{3-\delta}$	2.6	—	—	—	—	—

Dashes denote that the corresponding parameters were not determined.

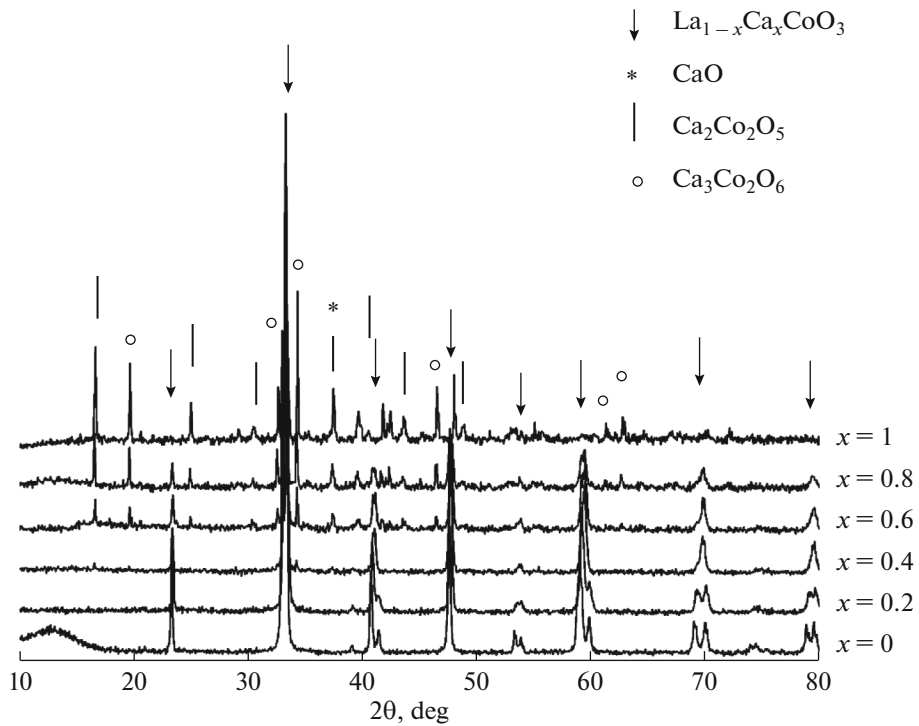


Fig. 3. X-ray diffraction patterns of the samples of $\text{La}_{1-x}\text{Ca}_x\text{CoO}_{3-\delta}$ before catalytic tests.

perature occurred gradually: the first low-temperature peak appeared at $\sim 400^\circ\text{C}$, and the second high-temperature peak appeared at about 600°C . With increasing x , the former peak was split and its intensity increased, and the temperature of the onset of reduction decreased. These changes were also characteristic of the high-temperature peak; this fact indicated the

improved reducibility of the samples with increasing x . According to Futai and Yonghua [25], the reduction of cations $\text{Co}^{3+} \rightarrow \text{Co}^{2+}$, $\text{Co}^{4+} \rightarrow \text{Co}^{2+}$, and $\text{Co}^{4+} \rightarrow \text{Co}^0$ occurred at temperatures to 500°C , and the reduction $\text{Co}^{2+} \rightarrow \text{Co}^0$ occurred above 500°C . We calculated the absorption of hydrogen in the regions corresponding to different steps of the reduction of samples by analogy with previously published data [26].

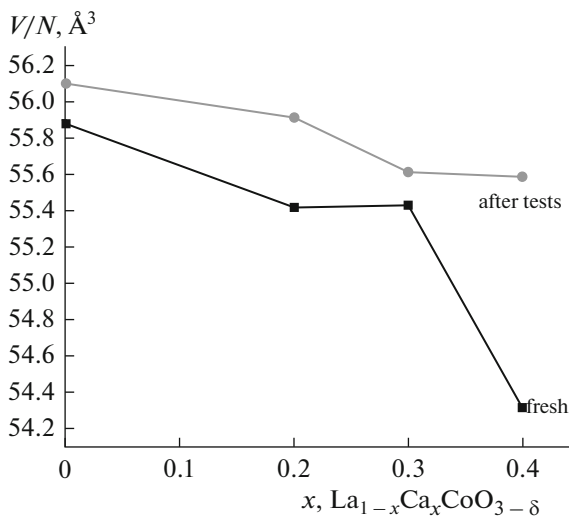


Fig. 4. Changes in the unit cell volume of the samples before and after tests depending on the calcium content (x) of the $\text{La}_{1-x}\text{Ca}_x\text{CoO}_{3-\delta}$ oxides.

The data given in Fig. 7 are indicative of an increase in the absorption in regions of both of peaks and in the

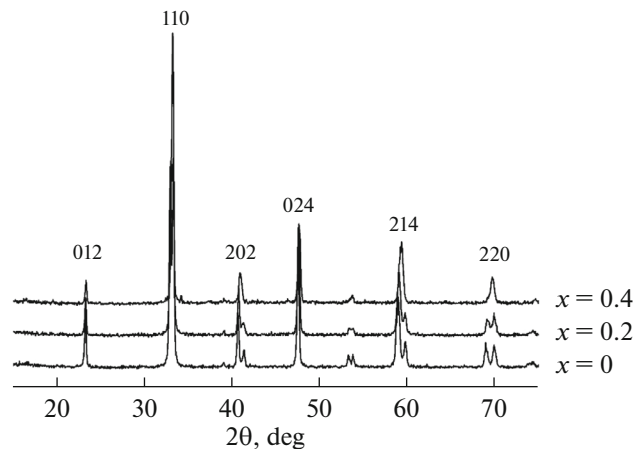


Fig. 5. X-ray diffraction patterns of the samples of $\text{La}_{1-x}\text{Ca}_x\text{CoO}_{3-\delta}$ after catalytic tests.

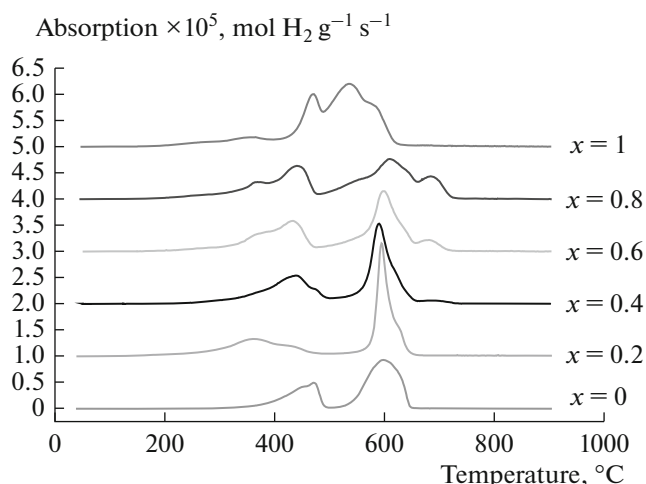


Fig. 6. TPR-H₂ curves of the samples of La_{1-x}Ca_xCoO_{3-δ}.

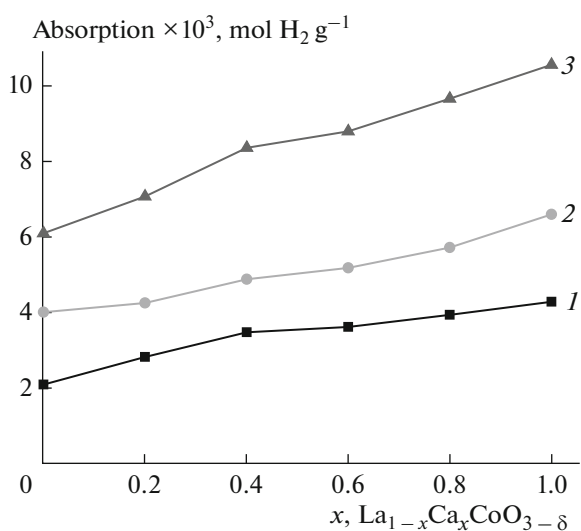


Fig. 7. Dependence of the amount of absorbed hydrogen on the composition of samples for the TPR-H₂ regions of (1) 20–500, (2) 500–900, and (3) 20–900°C.

total absorption of hydrogen by the samples and hence of an increase in the oxygen content of them. In accordance with the electroneutrality principle, this should lead to an increase in the charge on a portion of cobalt cations; that is, to an increase in the quantity of Co⁺⁴ cations with an increase in the calcium content (x) or to a decrease in the charge on oxygen ions.

The results obtained indicate that the samples were almost completely oxidized at room temperature (the vacancies were occupied with oxygen), and the removal of a portion of weakly bound oxygen and an increase of the quantity of vacancies in the oxides can occur in the reaction atmosphere with increasing the test temperature.

According to the transmission electron microscopy data described in detail by Gerasimov et al. [27], the particles of perovskite with $x = 0–0.2$ (LaCoO_{3-δ} and La_{0.8}Ca_{0.2}CoO_{3-δ}) were well-crystallized, round-shaped, and micron-sized. Starting with $x = 0.3$ (Fig. 8a), the particles of calcium oxide with sizes 5–20 nm were detected on the surface of the perovskite particles. It is likely that the small particle size of CaO did not make it possible to detect this phase by XRD analysis. The sample of La_{0.6}Ca_{0.4}CoO_{3-δ} consisted of polycrystalline lamellar particles with a smaller size of crystallites than that in the above samples; this can be related to a changed symmetry group. The particles of this composition were also characterized by coating with a layer of CaO on the surface of a perovskite phase (Fig. 8b).

After tests in the reaction of methane oxidation, the particles of perovskite in the samples with $x = 0–0.2$ (LaCoO_{3-δ} and La_{0.8}Ca_{0.2}CoO_{3-δ}) retained rounded well-crystallized shapes; however, structurally different locally ordered regions appeared in them: regions with increased interplanar spacing typical of orthorhombic oxide (a high-temperature modification) in the sample with $x = 0$; planar defects in the sample with $x = 0.2$ (Fig. 9a); and superstructurally ordered regions (structural fragments of brownmillerite Ca₂Co₂O₅ and perovskite–brownmillerite phase boundaries) in the particles of perovskite with $x = 0.4$ (Fig. 9b). In this case, the surfaces of all calcium-containing perovskite particles after tests were covered with a CaO layer to 20 nm in thickness. The particles of Co₃O₄ with sizes of 5–10 nm were also present [27].

The electron microscopic data indicated the instability of the La_{1-x}Ca_xCoO_{3-δ} solid solutions obtained in a methane-containing reaction atmosphere at temperatures to 600°C and the formation of planar defects in the perovskite structure, apparently, as a result of the ordering of both cationic and anionic vacancies, which were formed because of the partial degradation of oxides and the outcrops of calcium and cobalt oxides on the surface of the particles. Note that, obviously, a rearrangement occurred in the relatively thin near-surface layers of the perovskite phase because the X-ray diffraction patterns did not exhibit considerable changes to be indicative of the presence of new phases or planar defects in the bulk of perovskite phase particles. The formation of planar defects in the structures after catalytic tests was observed earlier in the near-surface layers of the perovskite particles of La_{1-x}Ca_xMnO_{3-δ} [10] and La_{1-x}Ca_xFeO_{3-δ} [20, 24] prepared by the Pechini method.

The above results make it possible to relate the pronounced decrease in the activity of a sample with $x = 0.3$ observed in the course of tests to the appearance of planar defects in the structure of perovskite and to the formation of a calcium oxide layer, which is not active in a deep oxidation reaction, on the surface of the particles. Because planar defects were also formed in the

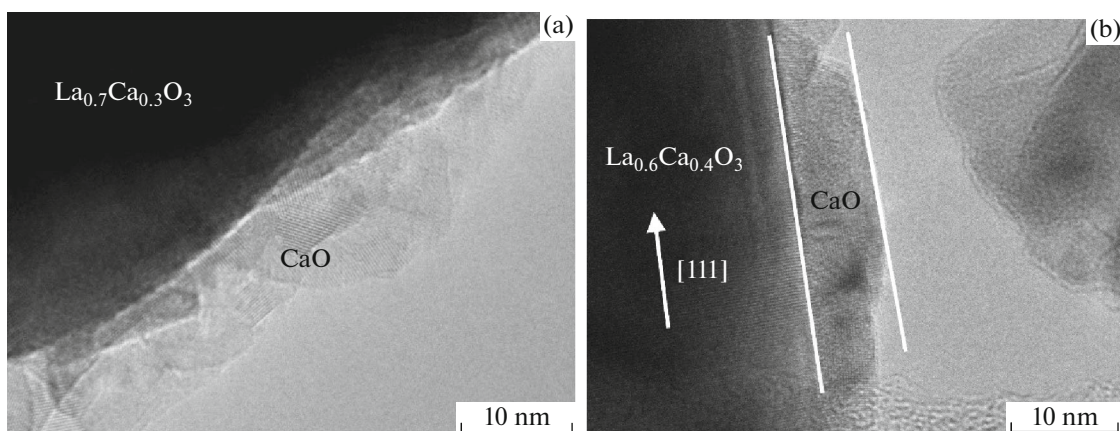


Fig. 8. Micrographs of the samples of (a) $\text{La}_{0.7}\text{Ca}_{0.3}\text{CoO}_{3-\delta}$ and (b) $\text{La}_{0.6}\text{Ca}_{0.4}\text{CoO}_{3-\delta}$ before testing in the reaction of methane oxidation.

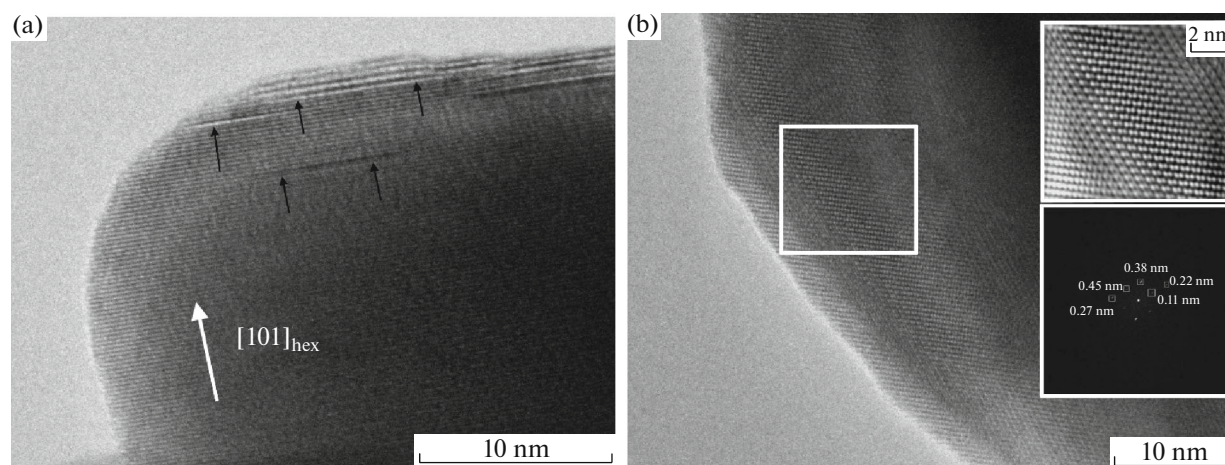


Fig. 9. Micrographs of the samples after testing in the reaction of methane oxidation: (a) the microstructure of $\text{La}_{0.8}\text{Ca}_{0.2}\text{CoO}_{3-\delta}$ (black arrows show planar defects in the direction of the crystal faces (101)); (b) the microstructure of $\text{La}_{0.6}\text{Ca}_{0.4}\text{CoO}_{3-\delta}$ (inserts show the filtered image and the Fourier transform of the chosen region to illustrate the presence of perovskite–brownmillerite phase boundaries).

particles of a sample with $x = 0.4$, but a layer of calcium oxide was present on its surface before the tests in contrast to the sample with $x = 0.3$, it is likely that an increase in the quantity of calcium oxide did not qualitatively change the surface composition and, correspondingly, did not exert a noticeable effect on its activity. Thus, the decrease in the activity of the sample with $x = 0.3$ observed in the course of reaction was mainly caused by the formation of calcium oxide on the surface layer, whereas the lower and stable activity of the sample with $x = 0.4$ was explained by the presence of a calcium oxide layer and a brownmillerite impurity phase in the initial oxide.

The observed increase in the initial catalytic activity of the samples upon the introduction of calcium to a value of $x = 0.3$ can be caused by an increase in the

quantity of weakly bound oxygen (Fig. 7), and the lowered activity of the samples with $x \geq 0.4$ was, probably, related to the presence of a less active vacancy-ordered phase of $\text{Ca}_2\text{Co}_2\text{O}_5$ on the surface.

Thus, the higher stability of samples with low ($x = 0-0.2$) or high ($x = 0.4-0.8$) degrees of substitution in a reaction atmosphere becomes clear because either few vacancies were formed in them or they already contained less active phases of $\text{Ca}_2\text{Co}_2\text{O}_5$ and CaO . With increasing the degree of substitution accompanied by an increase in the concentration of oxygen vacancies in the oxides after increasing the catalytic process temperature, their ordering occurred and manifested itself in the formation of vacancy-ordered structures (planar defects) in the structure of perovskite and the release of calcium oxide onto the sur-

face. Indeed, the degree of deactivation of the sample with $x = 0.3$ was higher than that of the samples with $x < 0.3$ (Fig. 2). Taking into account this tendency, we can also assume that the lower activity of the samples with $x = 0.4$ – 0.8 , which initially contained the impurity phases of $\text{Ca}_2\text{Co}_2\text{O}_5$ and CaO , was due to the fact that new phases did not appear under the action of a reaction atmosphere. It is possible that a certain decrease in the activity of these samples in the course of tests was related to changes in both the phase of perovskite and the impurity phase of $\text{Ca}_2\text{Co}_2\text{O}_5$ because the activity of the sample with $x = 1$ also decreased under the action of the reaction atmosphere.

The experimental data indicate that solid solutions based on the $\text{La}_{1-x}\text{Ca}_x\text{CoO}_{3-\delta}$ with $x > 0.2$ in a methane-containing reaction atmosphere were unstable even at a temperature of 600°C , and they decomposed with the formation of vacancy-ordered fragments in the perovskite structure and the release of calcium oxide onto the surface. Note that the decomposition of perovskites in the reaction atmosphere containing methane and oxygen differed from that in the case of heating in nitrogen. In the oxygen-free atmosphere, the decomposition of perovskite occurred with the release of CoO . The observed increase in the activity of oxides upon the introduction of calcium to $x = 0.3$ and changes in them under the action of a reaction atmosphere can be described in terms of changes in the quantity of vacancies and their ordering primarily in the near-surface layers of perovskite particles.

CONCLUSIONS

The study of the $\text{La}_{1-x}\text{Ca}_x\text{CoO}_{3-\delta}$ oxides prepared by the Pechini method showed that almost single-phase oxides were formed only to the values of $x = 0.4$, and the sample with $x = 0.4$ contained the impurity phases of $\text{Ca}_2\text{Co}_2\text{O}_5$ with the structure of brownmillerite and calcium oxide. The catalytic activity of the samples depends not only on their composition but also on the action of a reaction atmosphere. The activity of homogeneous solid solutions (in the region of $x = 0$ – 0.4) passed through a maximum with increasing x ; this can be due to both the presence of two polymorphous modifications in the sample with $x = 0.3$ and the presence of the less active phases of calcium cobaltite and calcium oxide in the sample with $x = 0.4$. The partial degradation of the perovskite phase accompanied by the formation of planar defects in the structure of perovskite and the release of calcium oxide occurred under the action of a reaction atmosphere in the near-surface layers of the solid solutions. Obviously, this was related to changes in the oxygen content of the perovskites. Therefore, the above processes of perovskite degradation can cause the observed

decrease in the activity of the samples in the course of tests in the reaction of methane oxidation.

ACKNOWLEDGMENTS

We are grateful to V.A. Rogov for the acquisition of the TPR- H_2 data.

This work was performed within the framework of a state contract at the Boreskov Institute of Catalysis, Siberian Branch, Russian Academy of Sciences (project no. AAAA-A17-117041710090-3).

REFERENCES

- Malkhand, S., Yang, B., Manohar, A.K., Manivannan, A., Prakash, G.S., and Narayanan, S.R., *J. Phys. Chem. Lett.*, 2012, vol. 3, no. 8, p. 967.
- Setevich, C., Moggi, L., and F. Prado, F., *Electrochem. Soc.*, 2012, vol. 159, no. 1, p. B72–B79. doi 10.1149/2.043201jesJ
- Solid state electrochemistry II. Electrodes, interfaces and ceramic membranes*, Kharton, V.V., Ed., Wiley-VCH, 2011, p. 576.
- Isupova, L.A., Sadykov, V.A., Ivanov, V.P., Rar, A.A., Tsybulya, S.V., Andrianova, M.A., Kolomiichuyk, V.N., Petrov, A.N., and Kononchuk, O.F., *React. Kinet. Catal. Lett.* 1994, vol. 53, 1, p. 223.
- Merino N.A., Barbero B.P., Cellier C., Gamboa J.A., and Cadús L.E., *Catal. Lett.*, 2007, vol. 113, no. 3–4, p. 130.
- Wu, Y., Yu, T., Dou, B.-S., Wang, C.-X., Fan, X.-R., and Wang, L.-C., *J. Catal.*, 1989, vol. 120, p. 88.
- Luu, T.H., Dung Nguyen, X., Huyen Phan, T.M., Schulze, S., and Hietschold, M., *Adv. Nat. Sci.: Nanosci. Nanotechnol.*, 2015, vol. 6, no. 2, p. 025016. doi 10.1088/2043-6262/6/2/025016
- Wong, Ng.W., Lawz, W.J., and Yan, Y.G., *Solid State Sci.*, 2013, vol. 17, p. 107.
- Cherepanov, V.A., Gavrilova, L.Ya., Barkhatova, L.Yu., Voronin, V.I., Trifonova, M.V., and Bukhner, O.A., *Ionics*, 1998, vol. 4, p. 309.
- Gavrilova, L.Ya., Cherepanov, V.A., Surova, T.V., Baimistruk, V.A., and Voronin, V.I., *Russ. J. Phys. Chem. A*, 2002, vol. 76, no. 2, p. 210.
- Mastin, J., Einarsrud, M.-A., and Grande, T., *Chem. Mater.*, 2006, vol. 18, p. 1680.
- Kononyuk, I.F., Tolochko, A.S.P., Lutsko, V.A., and Anishchik, V.M., *J. Solid State Chem.*, 1983, 48, p. 209.
- Melo, D.S., Marinho, E.P., Soledade, L.E.B., Melo, D.M.A., Lima, S.J.G., Longo, E., Santos, I.M.G., and Souza, A.G., *J. Mater. Sci.*, 2008, vol. 43, p. 551.
- Pathak, S., Kuebler, J., Payzant, A., and Orliovskaya, N., *J. Power Sources*, 2010, vol. 195, p. 3612.
- Merino, N.A., Barbero, B.P., Grande, P., and Cadus, L.E., *J. Catal.*, 2005, vol. 231, p. 232.
- Merino, N.A., Barbero, B., Eloy, P., and Cadus, L.E., *J. Appl. Surf. Sci.*, 2006, vol. 253, p. 1489.

17. Kumar, D.A., Selvasekarapandian, S., Nithya, H., Leiro, J., and Masuda, Y., *Power Technol.*, 2013, vol. 235, p. 140.
18. Haas, O., Ludwig, Chr., Bergmann, U., Singh, R.N., Braun, A., and Graule, T., *J. Solid. State Chem.*, 2011, vol. 184, p. 3163.
19. Nadeev, A.N., Tsybulya, S.V., Belyaev, V.D., Yakovleva, I.S., and Isupova, L.A., *J. Struct. Chem.*, 2008, vol. 49, no. 6, p. 1077.
20. Gerasimov, E.Yu., Isupova, L.A., and Tsybulya, S.V., *MRS Bull.*, 2015, vol. 70, p. 291. doi 10.1016/j.materresbull.2015.04.041
21. Isupova, L.A., Kulikovskaya, N.A., Saputina, N.F., Tsybulya, S.V., and Gerasimov, E.Yu., *Kinet. Catal.*, 2015, vol. 56, no. 6, p. 770. doi 10.7868/S0453881115050093
22. Isupova, L.A., Gerasimov, E.Yu., Zaikovskii, V.I., and Tsybulya, S.V., *Kinet. Catal.*, 2011, vol. 52, no. 1, p. 106.
23. Gerasimov, E.Yu., Zaikovskii, V.I., Tsybulya, S.V., and Isupova, L.A., *Poverkhnost'. Rentgenovskie, Sinkhrotronnye i neitronnye issledovaniya*, 2009, no. 10, p. 10.
24. Isupova, L.A., Gerasimov, E.Yu., Zaikovskii, V.I., and Tsybulya, S.V., *Kinet. Catal.*, 2011, vol. 52, no. 1, p. 104.
25. Futai, M. and Yonghua, Ch., *React. Kinet. Catal. Lett.*, 1986, vol. 31, no. 1, p. 47.
26. Yakovleva, I.S., Isupova, L.A., and Rogov, V.A., *Kinet. Catal.*, 2009, vol. 50, no. 2, p. 275.
27. Gerasimov, E., Kulikovskaya, N., Chuvilin, A., Isupova, L., and Tsybulya, S., *Top. Catal.*, 2016, vol. 59, nos. 15–16, p. 1354. 10.1007/s11244-016-0661-4

Translated by V. Makhlyarchuk